Nanoscale

Accepted Manuscript

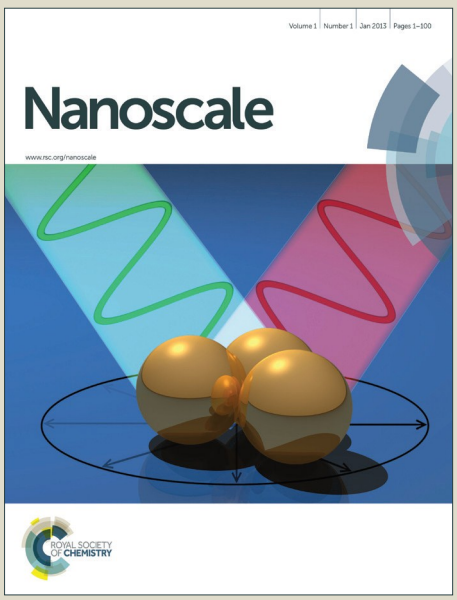

ROYAL SOCIETY OF CHEMISTRY

www.rsc.org/nanoscale

Journal Name

COMMUNICATION

Fabrication of Cubic Zn_2SnO_4/SnO_2 Complex Hollow Structure and Their Sunlight-Driven Photocatalytic Activity

Linqiang Sun,[a] Xiao Han,[a] Zhe Jiang,[a] Tingting Ye,[a] Rong Li,[a] Xinsheng Zhao,[b] Xiguang Han*[a]

Received 00th January 20xx,
Accepted 00th January 20xx

DOI: 10.1039/x0xx00000x

www.rsc.org/

Uniform hollow, yolk-shell and double-shell Zn_2SnO_4/SnO_2 nanoparticles with cubic morphologies have been synthesized using "etching – second growth – annealed" methods. Due to high light-harvesting efficiency and low recombination rate of photo-generated electron–hole pair, double-shell structures of Zn_2SnO_4/SnO_2 nanoparticles show an obvious improvement of photocatalytic activity.

Owing to environmentally friendly teachnology for the conversion of solar energy into chemical energy, sunlight-driven semiconductor photocatalysts have attracted worldwide attentions for their potentials in environmental and energy application.[1-6] In this context, intensive efforts have been devoted to design suitable materials to improve the photocatalytic efficiency, including the degree of light absorption, charge separation and surface reactivity. Recent progresses show that hollow structure materials present enhanced photocatalytic efficiency due to their multireflections of light, organic adsorption and porous characteristics.[7-14] Specifically, multiple-shell hollow structures with higher light adsorption efficiency exhibit superior performance to their conventional simple single-shelled counterparts in photocatalytic application.[15-18] As a result, many types of multi-shelled hollow structures metal oxide semiconductors have been fabricated through different synthesis methods.[19-25] For example, Qi et al. prepared triple-shelled CeO_2 hollow microspheres by using carbonaceous microspheres as hard templates, the performance in photo induced oxygen generation is 12 times higher than normal CeO_2 nanoparticles under UV irradiation.[20] Jang group fabricated multi-shell TiO_2 hollow nanospheres by employing silica spheres sacrificial template, it also shows an improvement in photocatalytic activity.[21]

Although hollow structure can enhance light-harvesting capabilities, high recombination rate between photo-generated electrons and holes is another major factor to reduce photocatalytic efficiency. Coupling of different semiconducting oxides with multi-bandgap or multi-junction has been widely studied and proved to have high quantum yield of electron-hole pair separation. Therefore, researcher are currently more focused on the design and fabrication of hollow structures with complexity composition to further improve their applications.[26-29] For example, Lou group developed a new "penetration-solidification-annealing" method to synthesize various mixed-metal-oxide multi-shelled hollow spheres.[28] Despite these advance to date, the development hollow structure with hybrid nanostructures remains as a significant challenge until now.

As an attractive n-type dual semiconducting oxide, Zn_2SnO_4 (ZTO) has high electron mobility, slower rate of electron–hole recombination and a longer lifetime of electrons than TiO_2.[30] When it couples with SnO_2 and used as photocatalytic materials, SnO_2 could act a sink for the photogenerated electrons because the conduction band (CB) position of ZTO is higher than that of SnO_2, which helps to increase the spatial separation of electron and hole, and thus enhance the efficiency of corresponding photocatalysis.[31-32] Recently, Lu et al. synthesized uniform ZTO/SnO_2 single-shell hollow spheres by calcining $ZnSn(OH)_6$ solid spheres in air, it shows good application in dye-sensitized solar cells.[33] However, it is still desirable to develop new efficient strategies to fabricate multi-shelled and non-sphered ZTO/SnO_2 hybrid nanostructures with high-performance photocatalytic activity.

Herein, we develop a etching and re-growth strategy to synthesize uniform cubic ZTO/SnO_2 single-shell, yolk-shell and double-shell hollow structure. When evaluated as photocatalytic materials, the double-shell hollow structure exhibits higher sunlight-driven photodegradation efficiency than other hollow structures.

[a] *Jiangsu Key Laboratory of Green Synthetic Chemistry for Functional Materials, Department of Chemistry, School of Chemistry and Chemical Engineering, Jiangsu Normal University, Xuzhou, 221116 (P. R. China). E-mail: xghan@jsnu.edu.cn.*
[b] *school of physics and electronic engineering, Jiangsu Normal University, Xuzhou, 221116 (P. R. China).*
† Footnotes relating to the title and/or authors should appear here.
Electronic Supplementary Information (ESI) available: [details of any supplementary information available should be included here]. See DOI: 10.1039/x0xx00000x

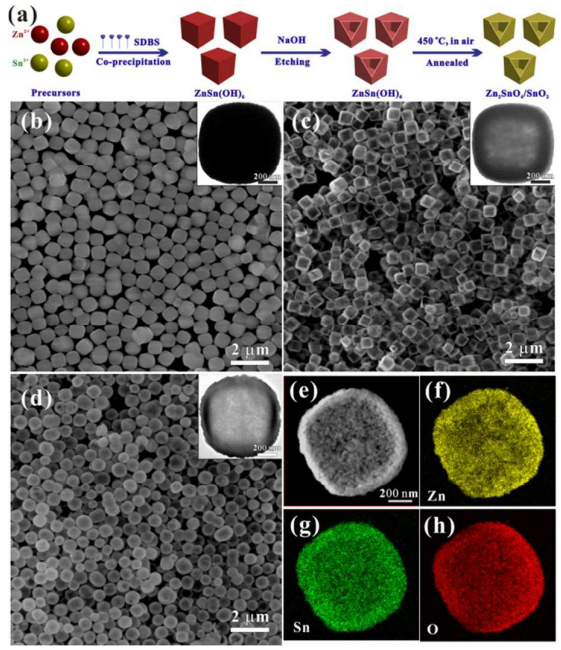

Fig. 1 (a) Schematic illustration of the formation mechanism of hollow Zn_2SnO_4/SnO_2 single-shell microboxes; SEM and TEM images of (b) $ZnSn(OH)_6$ solid cubes; (c) $ZnSn(OH)_6$ single-shell microboxes; (d) ZTO/SnO_2-SSNB; (e) Scanning TEM image; (f-h) elemental mapping images.

Our strategy for the formation of single-shell ZTO/SnO_2 single-shell microboxes is shown in Fig. 1a (the experimental detail are provided in the SI). In the first step, $ZnSn(OH)_6$ as the precursor are prepared by a facile solvothermal method. As show in Fig. 1b, the synthesized uniform $ZnSn(OH)_6$ cubes with smooth surface have a mean size of about 800 nm (length or width of particles), TEM image indicates the cubes are solid structures. According to the FTIR spectroscopy (Fig. S1), we can clearly see the sulfonic acid group peak. It indicates that the surface of particles adsorbs of sodium dodecylbenzenesulfonate (SDBS) in the process of crystal growth. Therefore, we think that SDBS adsorotion plays an important role in the formation of anisotropic ZnSn(OH)6 solid cubes (see SI file). The $Zn_2Sn(OH)_6$ solid cubes can be easily converted to single-shell $ZnSn(OH)_6$ microboxes by a simple NaOH etching process. The typical powder X-ray diffraction (XRD) shows that the products are still cubic-phase $ZnSn(OH)_6$ (JCPDS no. 00-020-1455) after etching treatment (Fig. S2). The morphologies of products are observed by field emission scanning electron microscopy (FE-SEM) and Transmission electron microscopy (TEM). As shown in Fig. 1c, the morphologies of products are uniform single-shell microboxes after etching process. TEM images (insert of Fig. 1b, Fig. S3) further confirm the hollow structure by the obvious contrast dark edges and the pale centre, and the shell thicknesses of the microboxes are in the range of 80 - 120 nm. The shell thickness can be controlled by changing the amount of NaOH, while the concentrations of the other reactants remain uncharged. Thicker shells would be achieved when less amount of NaOH are used(Fig. S4). After the annealing treatment at 450 ^{o}C, there exists a large weight loss (Fig. S5) and an obvious phase transition from $Zn_2Sn(OH)_6$ to mixed ZTO and SnO_2 phase (Fig. S2). The whole process of chemical reaction are shown in the supplementary information. From the SEM and TEM images (Fig. 1d), the morphology is preserved as highly uniform hollow single-shell nanoboxes. However, the diameter of ZTO is only around 700 nm, which is significantly smaller than that of $ZnSn(OH)_6$ microboxes because of the shrinkage during calcination process. The nitrogen adsorption/desorption isotherm of the ZTO/SnO_2 shows type II curve with Brunauer-Emmett-Teller (BET) specific surface area of 30 $m^2 \cdot g^{-1}$. To have a better understanding of the product composition, the scanning TEM (STEM) image with EDX elemental mapping and line scans are recorded in Fig. 1 e-h, Fig. S7. it can be seen that Zn, Sn and O elements are co-existence and homogeneous dispersion within the microboxes.

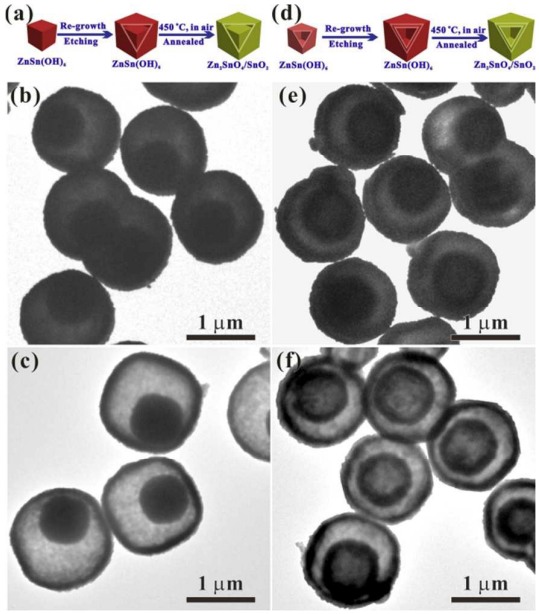

Fig. 2 (a) (d) Schematic illustration of the formation mechanism of Zn_2SnO_4 yolk-shell (a), and double-shell Structure (d); TEM image of yolk-shell structure, (b) $ZnSn(OH)_6$; (c) Zn_2SnO_4/SnO_2; TEM images of double-shell, (e) $ZnSn(OH)_6$; (F) Zn_2SnO_4/SnO_2.

Apart from single-shelled hollow particles, the solution synthesis of multishelled functional materials with non-sphered and hybrid nanostructures are fundamental challenge for synthetic chemistry due to a significant increase in structural complexity. The "etching-annealed" strategy can be further extended for the synthesis of Zn_2SnO_4/SnO_2 yolk-shell and double-shell structures. The synthesis process for making these unique structure is designed based on the repeated deposition of $ZnSn(OH)_6$ layers onto pre-grown seed particles such as microcubes and microboxs and subsequent alkaline etching and annealed process (Fig. 1a, d). When solid cubes are used as the seeds, TEM image (Fig. 2b) shows that the cubic morphology is perfectly retained and the formed $ZnSn(OH)_6$ cubes have a yolk –shell interior structure with a solid/hollow yolk. While the seeds change to single-shell microboxes, the double-shell microboxes with a porous/hollow yolk structures have been obtained (Fig. 2e). The crystal structure and phase purity are not altered in these hollow architectures as shown in XRD patterns (Fig. S8, S9). In the formation process of yolk-shell and double-shell structures, the dissolution of $ZnSn(OH)_6$ crystals mainly occurs between the passivated outer surface of seed particles and newly

deposited crystal layers, which are leading to the formation of yolk-shell and double-shell particles. However, the solid and hollow cubic shape of the seed particles can be well preserved during the new shell generated. After annealing treatment, $ZnSn(OH)_6$ precursor is completely converted to ZTO/SnO_2 hybrid microstructures (Fig. S8, S9, S10). The complex interior structure (yolk-shell, double-shell) are perfectly retained (Fig. 2c, f). The formation of core-shell structure possess higher BET surface areas (yolk-shell particles: 40 $m^2 g^{-1}$; double-shelled microboxes: 52 $m^2 g^{-1}$) than that of single-shell ZTO/SnO_2 microboxes (Fig. S11). Clearly, the high BET surface, unique structure and composition are beneficial for enhanced the photocatalytic properties.

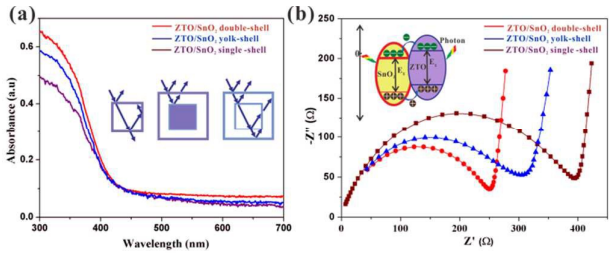

Fig. 3 (a) UV-vis diffuse absorption spectra of single-shell, yolk-shell and double-shell samples. The inset shows schematic illustration of multiple light reflections within the hollow structures; (b) Nyquist plots of three different hollow structures, inset is the schematic diagram of photocatalytic degradation over ZTO/SnO_2 catalyst under sun-light irradiation.

It is known that the optical properties of a semiconductor, which mainly include energy level and intensity of light absorption, are key factors in determining its photocatalytic activities. The UV-vis diffuse absorption spectra of single-shell, yolk-shell and double-shell samples are measured using a UV-vis spectrophotometer with an integrating sphere. As shown in Fig. 3a, all the samples exhibit spectral response near in visible range owing to the synergistic effect by charge-transfer transition between ZTO and SnO_2 conduction or valence in the hybrid sample.[32] Compared with single-shell, yolk-shell structures, double-shell structures exhibit higher light absorption, indicating that the incident light can be significantly scattered within the particles due to the double-shell structures, and the corresponding schematic is shown in the inset of Fig. 3a. Good performances of photocatalysis also depend on the high electrons and holes transport and separation efficiency. To investigate the differences in electron transport and recombination behaviors of the samples, the resistances are obtained through the corresponding Nyquist plots of the impedance data as shown in Fig. 3b. The semicircle in the EIS spectra is ascribed to the contribution from the charge transfer resistance (R_{ct}) and constant phase element at the photocatalyst/electrolyte.[34] The R_{ct} values of single-shell, yolk-shell and double-shell structures are 394, 306 and 250 Ω respectively. The low R_{ct} indicate the coupled system of semiconductors may slow down the recombination of photogenerated electrons and holes due to more efficient separation of electrons and holes (inset Fig. 3b). The above result also demonstrates that the transport of charge carriers (electron and hole) in double shell ZTO/SnO_2 is more facile than other hollow structures (yolk-shell and single-shell hollow structure). Considering the high BET surface, light-harvesting capabilities and improving mass transfer, double-shell ZTO/SnO_2 microboxes may exhibit high photocatalytic activity.

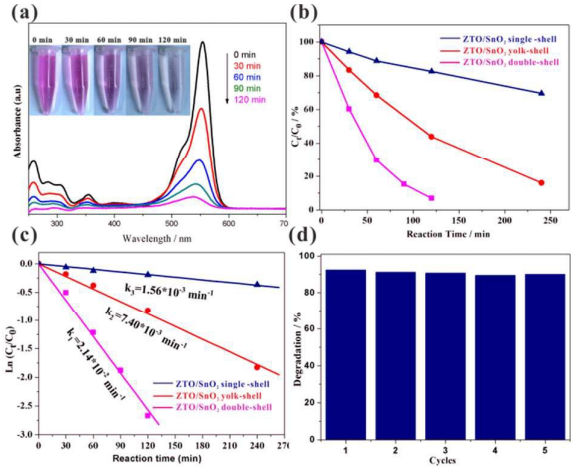

Fig. 4 (a) UV-vis absorption spectra of RhB as a function of sun-light irradiation time for double-shell ZTO/SnO_2 microboxes, the inset is corresponding photographs of RhB irradiated by sun light for different periods of time; (b) photocatalytic degradation curves of RhB over different photocatalysts; (c) plot of $\ln(C_t/C_0)$ as a function of time over different samples; (d) cycle stability of double-shell ZTO/SnO_2 catalysts.

Rhodamine B (RhB) is a common dye in the triphenylmethane family, which contains four N-ethyl groups at either side of the xanthene ring.[35] The photocatalytic activity of the hollow structure materials is evaluated by RhB degradation under sun light irradiation. As shown in Fig. 4a, when double-shell ZTO/SnO_2 microboxes are used as photocatalyst, the degradation could be almost finished within 120 min, and the photographs indicate that the solution change to be colourless after 120 min (inset Fig. 4a). The normalized temporal concentration changes (C_t/C_0) of RhB during the photocatalytic process are proportional to the normalized maximum absorbance (A_t/A_0), which can be derived from the change in the RhB absorption profile at a given time interval. Fig. 4b clearly shows that the photocatalytic activity of double-shell structure is higher than that of yolk-shell and single-shell structures. A linear relation of $\ln(C_t/C_0)$ versus reaction time is observe, implying that the photocatalytic reaction can be considered as a pseudo-first-order reaction (Fig. 4c). The double-shell ZTO/SnO_2 catalyst shows the fastest reaction rate, and the apparent kinetic rate constant is estimated to be $2.41*10^{-2}$ min^{-1}. In order to evaluate the catalytic stability, we carried out the cycle performance of double-shell structure ZTO/SnO_2 catalysts for degradation RhB under solar-light irradiation (Fig. 4d). The results reveal that the double-shell structures possesses outstanding catalytic stability and maintains above 95% in photodegration RhB after five cycle tests. After photocatalytic measurement, different structures Zn_2SnO_4/SnO_2 samples (single-shell, yolk-shell and double shell structures) have been characterized by SEM (Fig. S12). From the SEM images, we can see that the morphology of structures remain unchanged after photocatalytic measurement. Therefore, the enhanced photocatalytic activity of double-shell

structures should be mainly ascribed to increased light absorption due to enhanced multiple light reflections within the complicated interior cavity and reduced electron-hole pair recombination owing to the ZTO/SnO_2 hybrid nanostructures, which can be confirmed by UV-vis absorption and EIS measurements. Furthermore, the increased BET surface areas of double-shell structure should also contribute to the improvement of its photocatalytic performance.

In summary, we have developed a new and efficient strategy for synthesis of uniform ZTO/SnO_2 hollow cubes with complex interior structures (including single-shell, yolk-shell and double-shell structures). According to the UV-vis and EIS measurements, the double-shell ZTO/SnO_2 microboxes exhibit high light-harvesting capabilities and high electrons and holes transport and separation efficiency. As a result, owing to the specific structure, double-shell structures manifest super photocatalytic activity and stability under the sun-light irradiation.

Acknowledgements

This work was supported by the National Natural Science Foundation of China (Grant No. 21201088, 21376113), the Qing Lan Project and the Project Funded by the Priority Academic Program Development of Jiangsu Higher Education Institutions.

Notes and references

1 A. Hagfeldt, M. Gratzel, *Chem. Rev.,* 1995, **95,** 49.
2 M. R. Hoffmann, S. T. Martin, W. Choi, D. W. Bahnemann, *Chem. Rev.,* 1995, **95,** 69.
3 F. E. Osterloh, *Chem. Mater.,* 2008, **20,** 35.
4 A. Kudo, Y. Miseki, *Chem. Soc. Rev.,* 2009, **38,** 253.
5 X. Chen, S. Shen, L. Guo, S. S. Mao, *Chem. Rev.,* 2010, **110,** 6503.
6 G. Liu, J. C. Yu, G. Q. Lu, H. M. Cheng, *Chem. Commun.,* 2011, **47,** 6763.
7 H. Xu, S. X. Ouyang, L. Q. Liu, P. Reunchan, N. Umezawa, J. H. Ye, *J. Mater. Chem. A,* 2014, **2,** 12642.
8 H. Li, Z. Bian, J. Zhu, D. Zhang, G. Li, Y. Huo, H. Li, Y. Lu, *J. Am. Chem. Soc.,* 2007, **129,** 8406.
9 H. Qin, S. Wenger, M. Xu, F. Gao, X. Jing, P. Wang, S. M. Zakeeruddin, M. Gra tzel, *J. Am. Chem. Soc.,* 2008, **130,** 9202.
10 P. Guo, H. Song, X. Chen, *J. Mater. Chem.,* 2010, **20,** 4867.
11 X. Lai, J. E. Halpert, D. Wang, *Energy Environ. Sci.,* 2012, **5,** 5604.
12 J. B. Joo, I. Lee, M. Dahl, G. D. Moon, F. Zaera and Y. D. Yin, *Adv. Funct. Mater.,* 2013, **23,** 4246.
13 J. W. Nai, Y. Tian, X. Guan, L. Guo, *J. Am. Chem. Soc.,* 2013, **135,** 16082.
14 M. H. Oh, T. Yu, S. Yu, B. Lim, K. Ko, M. Willinger, D. Seo, B. H. Kim, M. G. Cho, J. Park, K. Kang, Y. Sung,1 N. Pinna, T. Hyeon, *Science,* 2013, **340,** 964.
15 N. N. Guan, Y. T. Wang, D. J. Sun and J. Xu, *Nanotechnology,* 2009, 20.
16 H. X. Li, Z. F. Bian, J. Zhu, D. Q. Zhang, G. S. Li, Y. N. Huo, H. Li, Y. F. Lu, *J. Am. Chem. Soc.,* 2007, **129,** 8406.
17 X. Wu, G. Q. Lu and L. Wang, *Energy Environ. Sci.,* 2011, **4,** 3565.
18 B. C. Liu, Q. Wang, S. L. Yu, P. Jing, L. X. Liu, G. R. Xu, J. Zhang, *Nanoscale,* 2014, **6,** 11887.
19 L. Zhang, H. B. Wu, X. W. Lou, *J. Am. Chem. Soc.,* 2013, **135,** 10664.
20 J. Qi, K. Zhao, G. D. Li, Y. Gao, H. J. Zhao, R. B. Yu, Z. Y. Tang, *Nanoscale,* 2014, **6,** 4072.
21 S. H. Hwang, J. Y. Yun, J. Jang, *Adv. Funct. Mater.,* 2014, **24,** 7619.
22 H. Hu, B. Y. Guan, B. Y. Xia, X. W. Lou, *J. Am. Chem. Soc.,* 2015, **137,** 5590.
23 L. F. Shen, L. Yu, X. Y. Yu, X. G. Zhang, X. W. Lou, *Angew. Chem. Int. Ed.,* 2015, **54,** 1868.
24 S. Lee, J. Lee, S. H. Hwang, J. Y. Yun, J. Jang, *ACS Nano,* 2015, **9,** 4939.
25 D. Zhang, J. Y. Zhu, Ni. Zhang, T. Liu, L. M. Chen, X. H. Liu, R. Z. Ma, H. T. Zhang, G. Z. Qiu, *Sci. Rep.*, 2015, **5,** 8737.
26 J. f. Qian, P. Liu, Y. Xiao, Y. Jiang, Y. l. Cao, X. P. Ai, H. X. Yang, *Adv. Mater.,* 2009, **21,** 3663.
27 J. Wang, X. Li, X. Li, J. Zhu, H. Li, *Nanoscale,* 2013, **5,** 1876.
28 G. Q. Zhang, X. W. Lou, *Angew. Chem. Int. Ed.,* 2014, **53,** 9041.
29 J. Wang, X. Y. Wang, X. L. Dong, X. F. Zhang, H. C. Ma, X. Fei, *RSC Adv.,* 2014, **4,** 59503.
30 B. Tan , E. Toman , Y. G. Li, Y. Y. Wu, *J. Am. Chem. Soc.,* 2007, **129,** 4162.
31 T. J. Coutts, D. L. Young, X. Li, W. P. Mulligan, X. Wu, J. Vac, *Sci. Technol. A,* 2000, **18,** 2646.
32 B. Li, L. Luo, T. Xiao, X. Hu, L. Lu, J. Wang, Y. Tang, *J. Alloy Compd.,* 2011, **509,** 2186.
33 R. M. Liu, W. Du, Q. Chen, F. Gao, C. Z. Wei, J. Sun, Q. Y. Lu, *RSC Adv.,* 2013, **3,** 2893.
34 H. C. Sun, L. K. Pan, W. Qin, T. Q. Chen, Z. Sun, *J. Mater. Chem. A,* 2013, **1,** 6388.
35 Q. Wang, C. C. Chen, D, Zhao, W. H. Ma, J. C. Zhao, *Langmuir,* 2008, **24,** 7338.

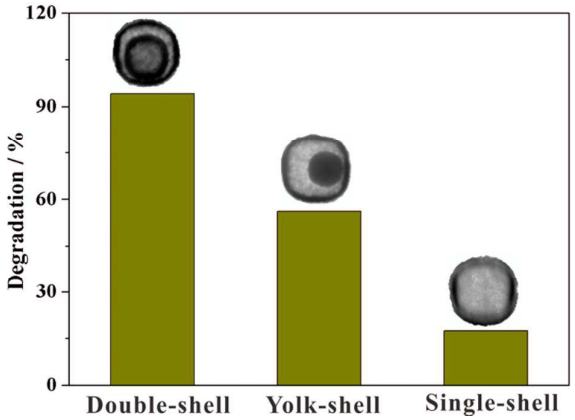

Uniform hollow, yolk-shell and double-shell Zn_2SnO_4/SnO_2 nanoparticles with cubic morphologies have been synthesized using "etching – second growth – annealed" methods. Double-shell structures of Zn_2SnO_4/SnO_2 nanoparticles show an obvious improvement of photocatalytic activity.